

Estimating Optical Properties of Layered Surfaces Using the Spider Model

Tetsuro Morimoto
Information Technology Research Laboratory,
Toppan Printing Co.,Ltd
tetsuro.morimoto@toppan.co.jp

Robby T Tan
Department of Information and Computing Sciences,
Utrecht University
robby@cs.uu.nl

Rei Kawakami Katsushi Ikeuchi
Institute of Industrial Science,
The University of Tokyo
{rei,ki}@cvl.iis.u-tokyo.ac.jp

Abstract

Many object surfaces are composed of layers of different physical substances, known as layered surfaces. These surfaces, such as patinas, water colors, and wall paintings, have more complex optical properties than diffuse surfaces. Although the characteristics of layered surfaces, like layer opacity, mixture of colors, and color gradations, are significant, they are usually ignored in the analysis of many methods in computer vision, causing inaccurate or even erroneous results. Therefore, the main goals of this paper are twofold: to solve problems of layered surfaces by focusing mainly on surfaces with two layers (i.e., top and bottom layers), and to introduce a decomposition method based on a novel representation of a nonlinear correlation in the color space that we call the “spider” model. When we plot a mixture of colors of one bottom layer and n different top layers into the RGB color space, then we will have n different curves intersecting at one point, resembling the shape of a spider. Hence, given a single input image containing one bottom layer and at least one top layer, we can fit their color distributions by using the spider model and then decompose those layered surfaces. The last step is equivalent to extracting the approximated optical properties of the two layers: the top layer’s opacity, and the top and bottom layers’ reflections. Experiments with real images, which include the photographs of ancient wall paintings, show the effectiveness of our method.

1. Introduction

The surface of most natural objects contains a number of layers with different physical substances. For instance, human skin is composed of at least two layers: epidermis and dermis. Each of these layers has distinct optical properties,

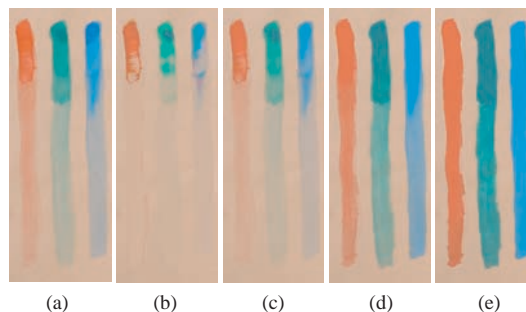


Figure 1. The two-layered surfaces of water colors: (a) Real input image. (b) Simulation by reducing the opacity of the original 10%, (c) by reducing 50%, (d) by increasing the opacity 3 times, and (e) by increasing 9 times.

such as opacity and reflectance, and this kind of surface is known as layered surfaces. The total reflection from such a surface, and therefore its appearance, is determined by those optical properties. As an illustration, let us consider a two-layered surface with different colors. The appearance of the surface is the mixture of the colors governed by the opacity of the top layer. If the opacity changes gradually across the surface, then the mixture of the colors will change accordingly, as depicted in Fig. 1. a. Other examples of layered surfaces are leaves, biological tissues, patinas, and some paintings including wall paintings.

To decompose such surfaces and to extract each layer’s optical properties will be beneficial to many research fields, such as archaeology, biology, and medical fields. For example, if we have ancient wall paintings in which some of the parts are degraded (but not totally removed) due to weather and time, and we have to recover those parts, then we need to extract the top layer (the painting layer) from the bottom layer (the wall layer). Having extracted the optical prop-

erties, we can generate various simulated images based on different opacities. This is illustrated in Fig. 1. Similarly, this technique can be used to decompose other layered surfaces.

Many models of layered surfaces have been introduced [2, 21, 6, 3] that rely on radiative transfer theory. One highly detailed representation is the many-flux scattering model presented by Mudgett [11]. However, the model is too complex and cannot be applied to our problem setting. In color science and computer vision, there are two simpler models that are frequently used: the Kubelka-Munk (KM) model [7] and the Lambert-Beer (LB) law [1]. The KM model is explicitly based on two flux scattering models, while the LB law is based on the exponential function of the attenuation factor. Both of them are approximated models. In the computer vision community, many papers [13, 12, 15, 5, 17] extend the LB law into a linear combination of transmissions and reflections, which we call the LB-based model. The KM model is more complex than the LB-based model and is supposed to be more accurate. However, in our experiments, we found that the KM model is more susceptible to noise. Hence, this paper uses the LB-based model.

The goal of this paper is to extract the optical properties of layered surfaces with two layers (i.e., top and bottom layers). We intend to extract the opacity of the top layer and the reflection of both layers using the LB-based model. The extraction implies the decomposition of the two layers. To attain our goal, we will use a “spider” model, a novel representation of a nonlinear correlation in the color space. The reason we call it the spider model is because, when we plot the RGB values of the mixtures of one bottom layer and n different top layers into the color space, then we will have n different curves intersecting at one point, resembling the shape of a spider. This shape can be derived from the LB-based model, mathematically. Hence, given a single input image containing one bottom layer and at least one top layer, we can fit the spider model to their color distributions and then decompose those layered surfaces.

A number of approaches used in digital matting are related to this paper, since the LB-based model happens to be similar to a model used in digital matting that is known as the alpha-matting equation. The goal of digital matting is to extract foreground objects from the background, and therefore is about estimating the degree of a pixel occupied by foreground objects. There are several types of digital matting. Poisson-based matting [18] resolves the problem by using the gradients of the opacity and solving the partial differential equation. Robust matting [20] proposes a robust global sampling method, assisting the local sampling procedure to generate a sufficient number of color samples. Closed-form matting [8] and spectral matting [9] assume foreground and background colors can be fitted with a linear color line model in local windows, which leads to a

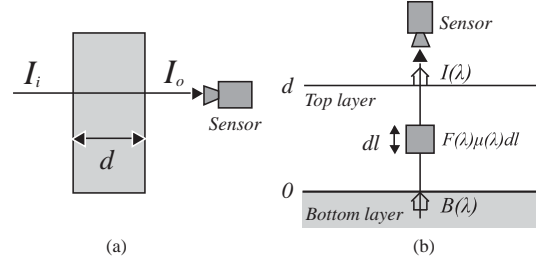


Figure 2. (a) The optical model of the Lambert-beer model. (b) The optical model based on the Lambert-Beer model of layered surface objects

quadratic cost function in alpha that can be minimized globally. Other methods of digital matting are [4, 16]. Almost all of these matting methods assume that color change appears to be a line in RGB space, since the occupancy of foreground objects equally affects RGB channels. However, for layered surfaces, color change becomes a curved line in RGB space. This is one of the main differences between the alpha-matting equation and our model.

This difference is also true of the group of papers by S. K. Nayar’s group that initiated an area referred to as bad weather. The representative examples include enhancement of visibility in atmospheric imagery [13, 12, 15, 5]. In these papers, the researchers consider color mixture caused by a layer of water drops. Since the attenuation caused by a water drop is close to gray, like in the alpha-matting equation, the color mixture in their problem setting can be assumed to be linear in RGB space.

In computer graphics, several models have been proposed to visualize layered surfaces and their scattering properties, such as human skin and subsurface scattering [8,6,3]. However, they are intended for the purpose of visualization, and too complex to be used in computer vision frameworks.

The structure of the remainder of this paper is as follows: in Section 2, we discuss the model used in our method. In Section 3, the spider model, which is the core of our decomposition technique, is explained in detail. In Section 4, we apply the spider model to estimate two-layered surfaces. In Section 5, we show how to simulate different opacities, rendering different appearances of a layered surface. We discuss the experimental results in Section 6, and in Section 7, we discuss our framework. Finally, in Section 8, we conclude our paper.

2. Layered Surface Model

The optical transmittance of light passing through a transparent object can be described by the Lambert-Beer Law [1]. It is the exponential function of the attenuation factor multiplied by the distance of the light traveling through

the object, which is written as:

$$T(\lambda) = \frac{I_o(\lambda)}{I_i(\lambda)} = e^{-\mu(\lambda)d}, \quad (1)$$

where T is the optical transmittance, λ is the wavelength, I_o is the intensity of the outgoing light, I_i is the intensity of the incoming light, μ is the attenuation factor of the object, and d is the distance of the light traveling through the object (the length of the light path). Assuming the light travels perpendicularly to the object surface, d can represent the optical thickness of the object. Fig. 2. a shows the pictorial description of the law.

The light reflected from layered surfaces can be modeled based on the Lambert-Beer law, which in this paper we call the Lambert-Beer based model, or LB-based model. First, let us consider the reflection from the bottom layer. The light reflected from the bottom layer is attenuated during the travel through the top layer; thus, the light received by the sensor becomes $B(\lambda)e^{-\mu(\lambda)d}$ from Eq. (1). B is the reflected light at the bottom layer, μ is the attenuation of the top layer, and d is the thickness, as illustrated in Fig. 2. b.

The light that is reflected by pigments of the top layer in the infinitesimal distance dl is $F(\lambda)\mu(\lambda)dl$, according to the definition of attenuation [13]. Here, we assume that pigments receive the same amount of light F in the top layer. The total amount of light reflected by the top layer is the sum of the light coming from each infinitesimal distance dl , which is the integration over the distance d : $\int_0^d F(\lambda)\mu(\lambda)e^{-\mu(\lambda)l}dl = F(\lambda)(1 - e^{-\mu(\lambda)d})$. Note that each light from dl is attenuated by the factor of $e^{-\mu l}$ by other pigments.

Thus, the total amount of light observed by the sensor becomes

$$I(\lambda) = B(\lambda)e^{-\mu(\lambda)d} + F(\lambda)(1 - e^{-\mu(\lambda)d}), \quad (2)$$

where I is the mixture intensity of the transmitted light from bottom and top layers. We call I a mixed layer. B and F can also be defined as the intensity of light coming from the surface when the thickness d is zero and infinitely large (∞), respectively. In this paper, we define opacity $\phi(\lambda) = 1 - e^{-\mu(\lambda)d}$. Hence, if we have two-layered surfaces, they are composed of the bottom layer $B(\lambda)$, the top layer $F(\lambda)$, and the opacity of the top layer $\phi(\lambda)$. This paper assumes that the opacity of the bottom layer is infinitely large throughout the image.

In more details, there are two types of bottom layers. The first is the bottom layer that is not covered by the top layer. This bottom layer receives light directly from the light source, which mathematically can be described as:

$$B'(\lambda) = L(\lambda)\rho(\lambda), \quad (3)$$

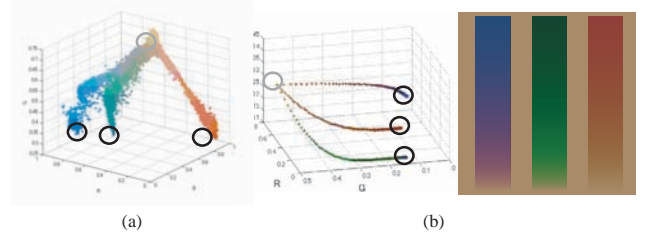


Figure 3. Spider model: (a) The plot of Fig. 1. a into the normalized color space. The gray circle represents the bottom layer's reflection. Black circles represent the top layer's reflection with the largest opacity value. (b) Left side: simulation of spider model using LB-based model. We plotted three colors with various opacity values. The gray circle represents the bottom layer's reflection. Black circles represent the top layer's reflection when the opacity=1. Right side: the simulated image.

where B' is the reflection of the bottom layer when it is not covered by the top layer. L is the light intensity. ρ is the albedo of the bottom layer.

The second type is the bottom layer covered by the top layer, which we can formulate as:

$$B(\lambda) = L(\lambda)e^{-\mu(\lambda)d}\rho(\lambda), \quad (4)$$

and differs from Eq. (3) due to the change of the light impinging on its surface ($L(\lambda)e^{-\mu(\lambda)d}$). Note that in the last equation, we ignore the cumulative reflections reflected back and forth from the bottom layer to the top layer (the interface reflections), since we assume that the top layers are sufficiently thin.

3. Spider Model

Pixel values of a layered surface distribute as a curved line in the RGB space. They resembles the shape of a spider when multiple lines are observed. This section introduces the spider model and shows the derivation of it using the LB-based model (Eq. (2)).

Let us start with an example. Fig. 3. a shows the plot of Fig. 1. a into the RGB space. As one can observe, the three top layers roughly form three non-linear lines in the space. They stretch from the pixel values that represent the top layers with the largest opacity to the pixel values representing top layers with less and less opacity, and end up by intersecting at the bottom layer where the opacities of the three top layers equal zero. Fig. 3. b shows a synthetic image generated by the LB-based model (right), and its plot into the color space (left).

Mathematically, we derive the spider model as follows. First, instead of using spectral data, we use RGB color data taken from an ordinary digital camera for which the gamma correction is set to off. The LB-based model for the RGB

data, then, can be expressed as:

$$I_c(x) = B_c(x)e^{-\mu_c(x)d(x)} + F_c(x)\left(1 - e^{-\mu_c(x)d(x)}\right), \quad (5)$$

where index c represents one of the three color channels $\{r, g, b\}$ and x is the spatial image coordinate. B_c is the reflection by the bottom layer. F_c is the reflection of the top layer when the thickness is infinitely large (or sufficiently large so that the bottom layer does not affect the top layer's reflection). In the last equation, we assume that the camera's color sensitivities follow the Dirac delta function. For the sake of simplicity, we will omit x throughout the paper; however, unless it is stated otherwise, the variables should be considered to be dependent on x .

Considering the intensities in the red and green color channels, from Eq. (5), we can write:

$$I_r = B_r e^{-\mu_r d} + F_r (1 - e^{-\mu_r d}) \quad (6)$$

$$I_g = B_g e^{-\mu_g d} + F_g (1 - e^{-\mu_g d}). \quad (7)$$

In the two equations, all variables are dependent on the color channels except for d . Thus, by letting $\alpha_c = e^{-\mu_c d}$:

$$-d = \frac{\ln(\alpha_c)}{\mu_c} \quad (8)$$

$$\frac{\ln(\alpha_r)}{\mu_r} = \frac{\ln(\alpha_g)}{\mu_g} \quad (9)$$

$$\alpha_r = \alpha_g^{\mu_r/\mu_g}. \quad (10)$$

From Eq. (7), we know that:

$$\alpha_g = \frac{I_g - B_g}{F_g - B_g}. \quad (11)$$

Substituting the last equation into Eq. (10), we can obtain:

$$\alpha_r = \left(\frac{I_g - B_g}{F_g - B_g} \right)^{\mu_r/\mu_g}. \quad (12)$$

Finally, by plugging the last equation into Eq. (6), we can express the intensity of the red color channel as:

$$I_r = B_r + \psi_r (I_g - B_g)^{\gamma_r}, \quad (13)$$

where $\gamma_r = \mu_r/\mu_g$, and $\psi_r = (F_r - B_r)/(F_g - B_g)^{\gamma_r}$. Accordingly, we can apply to the blue color channels, resulting in the following equation:

$$I_b = B_b + \psi_b (I_g - B_g)^{\gamma_b}, \quad (14)$$

where $\psi_b = (F_b - B_b)/(F_g - B_g)^{\gamma_b}$, and $\gamma_b = \mu_b/\mu_g$. Eqs. (13) and (14) imply that the correlations of the intensities in different color channels are not linear. Fig. 3. a shows the plot of the intensities, I_c , of layered surfaces (Fig. 1. a)

in the RGB space, which form curved lines as predicted by Eqs. (13) and (14).

This spider model is the core of our method, since by obtaining it, we are able to know the optical parameters of the layered surface, which in turn enables us to classify the color of the top and bottom layers of a pixel. Furthermore, using their properties, we can analyze opacities of layers, and also simulate the color changing depending on the top layer's thickness as shown in Fig. 1.

4. Estimating Optical Properties of Layered Surfaces

Given a single input image containing the mixture of bottom and top layers, this section shows how to extract the optical properties of layered surfaces based on the spider model. This process is possible to be fully automatic, for example by tracing every line distribution in the color space, similar to [14]. However, in this paper, to show the effectiveness of the spider model, we utilize simple user interactions to brush rough areas where the top layers and background layers are present. The brushing (or scribbling) can be as simple as drawing a line, as shown in Fig. 4. b.

Overall, our proposed method consists of two processes: (1) Extracting the spider model (ψ_c, γ_c) , (2) Determining the value of B_c, F_c and ϕ_c of each pixel in the input image by using a graphical model. This process is similar to the problem of labeling pixels by using multiple labels.

4.1. Estimating Spider Model

The aim of this section is to discuss how we can extract the spider model's parameters (ψ_c, γ_c) . We consider two of cases: (1) an input image with a single bottom layer and several top layers, (2) an input image with several top layers and several bottom layers. Note that, these cases are just examples of conditions where our method can work.

Fig. 4. a shows an example of case 1. We assume that from the user's scribble we can have parts of regions where the top layers are present and parts of the bottom layer's region. To have the spider model's parameters of each region, we plot the pixels that correspond to the scribble on the top layer, producing three independent distributions in the RGB space as shown in Figs. 4. c - e. Fitting the spider model onto each of the distributions according to Eq. (13) and (14), will give us the values of $\{\psi_c, \gamma_c\}$ for red, green, and blue top layers. To help estimate $\{\psi_c, \gamma_c\}$, we use Levenberg-Marquardt method. The same process also works for an input image that has a single bottom and a single top layer. Note that B_c is known, since we can obtain it from the bottom region marked by a user.

Fig. 5. a shows an example of case 2, an input with several top layers and several bottom layers. For this case, not only can we estimate $\{\psi_c, \gamma_c\}$ for every top layer, but also estimate the values of F_c . Since according to the spider

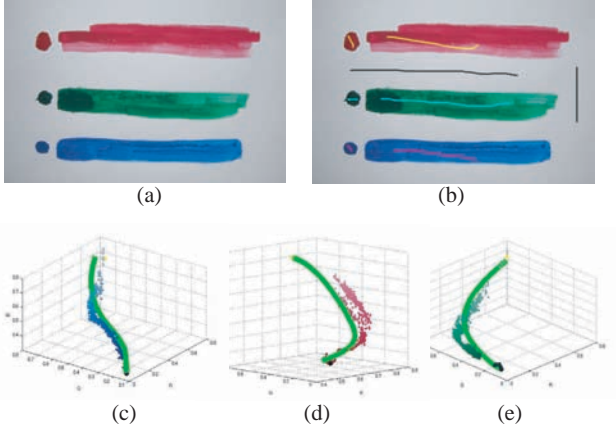


Figure 4. Estimated spider model: (a) Input image. (b) Marked regions. (c) Estimated line of blue. (d) Estimated line of red. (e) Estimated line of green.

model, if we have a top layer with two bottom layers, we will have two curve lines that intersect at a point representing opacity, $\phi_c = 1$. This phenomenon is shown in Fig.5. c until e. In the perspective of the spider model, the phenomenon also occur when we have two or more top layers and one bottom layer, where the intersection point indicates the reflection of the bottom layer B_c .

4.2. Layered Surface Decomposition

To decompose layered surfaces in an image is equivalent to estimating F_c , B_c , and ϕ_c for every pixel in the image. Therefore, given $\{I_x\}$, $\{B_c\}$, $\{w_l\}$, where index x represents an input-image pixel, I_x is the RGB values of pixel x , w_l is the curve line (or the spider’s leg) generated by $\{\psi_c, \gamma_c\}$ of top layer l , we intend to estimate the label of x . In our case, the number of labels depends on the number of the top layers and the bottom layers, which is defined as $L = [1, \dots, l, \dots, N + 1]$, where N is the number of the top layers, and $N + 1$ is because we include the label of the bottom layer. For clarity, in this section we assume that we only use one bottom layer, although the method discussed below can also work for multiple bottom layers.

Solving this problem is also equivalent to computing the probability of the label of a pixel based on the distance between the pixel’s RGB value and a leg of the spider model, where the leg represents the curve line that leads to the top layer. The closer the distance of a pixel to a leg, the higher the probability.

To correctly label the pixels, we should incorporate the case when a pixel is closed to the head of the spider model, meaning when a pixel is closed to a bottom layer. This can be solved by creating a data cost described as follows:

$$D(x = l | B_c, w_l, I_x) = \begin{cases} 0 & \text{if } d(I_x, B_c) < th \\ 1 - e^{-d(I_x, w_l)} & \text{otherwise} \end{cases} \quad (15)$$

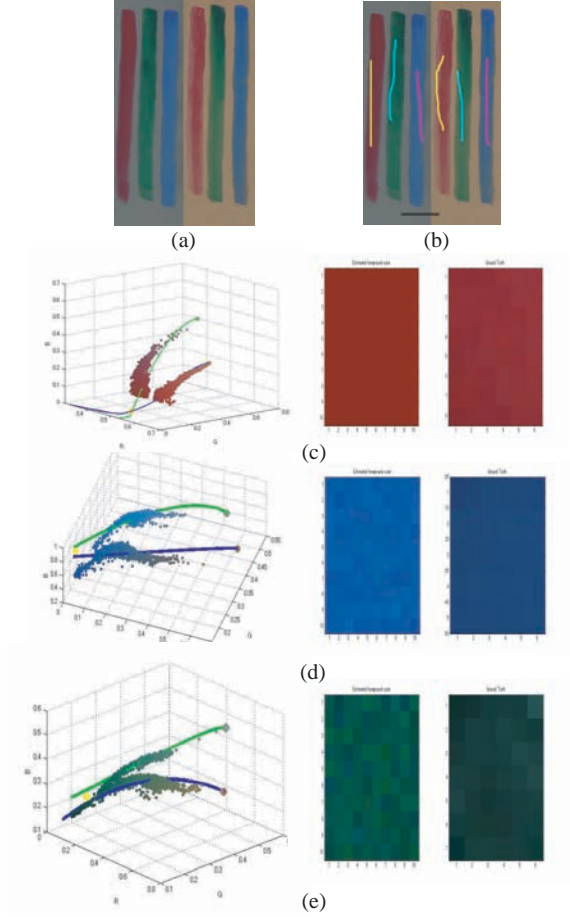


Figure 5. Estimated spider model using the intersection of color lines. (a) Input image. (b) Marked regions (c) Red: (left) Estimated color lines, (right) Estimated color of the top layer and ground truth. (d) Blue: (left) Estimated color lines, (right) Estimated color of the top layer and ground truth. (e) Green: (left) Estimated color lines, (right) Estimated color of the top layer and ground truth.

where B_c is the RGB value of a bottom layer. w_l represents the curved line created by parameter $\{\psi_c^l, \gamma_c^l\}$. Function d represents the Euclidean distance in the RGB space. Threshold th is set depending on the noise level of the bottom layer and the camera, in our experiment we set the value between $10 \sim 20$ (within RGB standard values from 0 to 255). As the initial values, for all values of i and x , we set $D(x = l | B_c, w_l, I_x) = 1$.

Next, we also employ the smoothness constraint, and model the spatial correlations based on MRFs:

$$E(\{x\}, \{B_c\}, \{w_l\}, \{I_x\}) = \sum_p D(x = l | B_c, w_l, I_x) + \sum_{p,q} S(x_p, x_q) \quad (16)$$

where $S(x_p, x_q)$ will be zero if $x_p = x_q$, and one other-

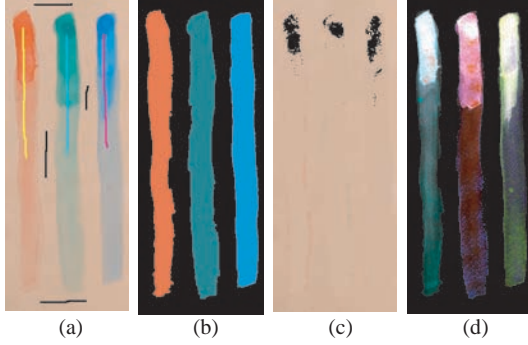


Figure 6. The result of layered surface decomposition: (a) Input image with user specified top and bottom strokes. (b) Extracted top layer's image. (c) Extracted bottom layer's image. (d) Extracted opacity image ($1 - e^{-\mu d}$).

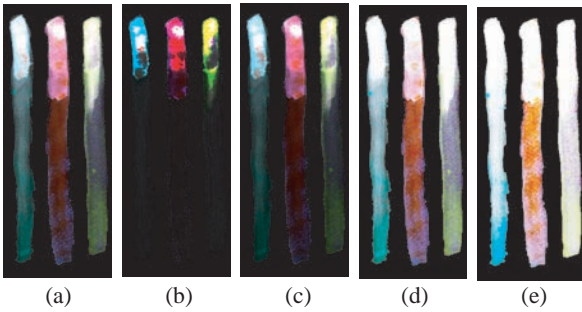


Figure 7. (a) Estimated opacity image. (b) Reducing the opacity with $n = 0.1$. (c) Reducing the opacity with $n = 0.5$. (d) Increasing the opacity with $n = 3$. (e) Increasing the opacity with $n = 9$.

wise. To minimize the cost function, we use graphcuts for multiple labels [19].

Having labeled every pixel, we can now estimate the values of F_c , by analyzing the pixel distribution that are labeled to a top layer. F_c is the pixel that has the largest geodesic distance from B_c , since they are the edge points of the distribution. Finally, having estimated the values of F_c , we can straightforwardly compute the values of ϕ_c (the opacity) for every pixel. The Figs. 6 show decomposed images of Fig. 1. a.

5. Simulation

Having decomposed the layers and extracted their optical properties, we are able to simulate the top layer's appearances with various degrees of opacity. If the estimated opacity image is represented as $\phi = 1 - e^{-\mu d}$, we can write: $e^{-\mu d} = 1 - \phi$. From Section 3, we know that if we increase the opacity, optically it means we increase the optical thickness of the object. Thus, increasing the thickness n times implies:

$$e^{-\mu nd} = (1 - \phi)^n. \quad (17)$$

Based on the last equation, we can simulate the opacity by using the following formula:

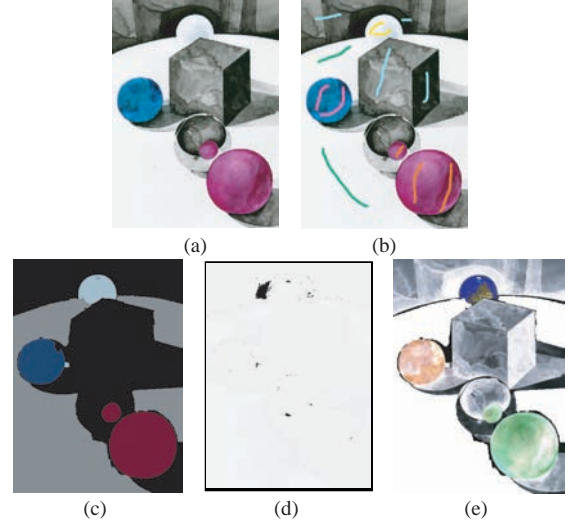


Figure 8. (a) Input image: a water color painting painted by a professional artist. (b) Input image with user-specified top and bottom strokes. (c) Extracted top layers. (d) Extracted bottom layer. (e) Extracted opacity image.

$$\phi' = 1 - (1 - \phi)^n, \quad (18)$$

where ϕ' is the simulated opacity, and n is a positive real number to change the thickness.

We simulated the opacity of the water color painting in Fig. 1.a. Fig. 7. a shows the original estimated opacity, while Figs. 7. b-e show various simulated opacities. These opacities correspond to the appearances of the water color shown in Figs. 1. a-e. Note that the opacity is dependent on the wavelength, thus different color channels give different opacities, making the appearance of the opacity not white.

6. Experimental Results

Setup In our experiment, we captured the images using NIKON DIX. The camera is radiometrically calibrated to obtain a linear correlation between the incoming light and the image intensities by setting the gamma correction off. We arranged the position of the light source distant from the objects, and we excluded the possibilities of shadows and interreflections. The regions of mixed layers and bottom layer in the captured image are roughly marked by user interaction. Then, optical properties of the layered surfaces are estimated.

Results First, we demonstrate the application of layered surface decomposition to a water color painting. Figs. 8. a and b show, respectively, the input image, and the regions marked by a user. The input image is a water color painting painted by a professional artist. The result of the estimated values of F_c for every pixel is shown in Fig. 8. c, which also represents the success of segmentation using a spider model. In Fig. 8. c, the region in gray is the pixels labeled

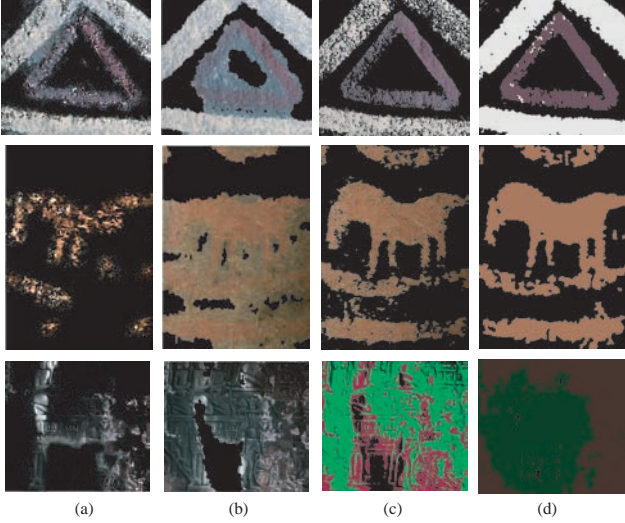


Figure 9. Segmentation of layered surfaces: (a) Closed-form matting [8]. (b) Lazy Snapping [10]. (c) K-means. (d) Our method.

as the bottom layer. Other colors represent the estimated top layer’s color of each pixel. Figs. 8. d and 8. e show the images of the bottom layer B_c and the estimated opacity ϕ , respectively. Fig. 8. d is white since it represents the white canvas.

Next, as the results of being able to increase opacity synthetically, we can apply our method to increase the accuracy and robustness of color segmentation, particularly for objects with layered surfaces. Here, we will show the results of our segmentation based on our layered surface decomposition compared with the closed-form matting [8], an object segmentation method [10] and a k-means method. Fig. 9 shows the segmentation results of applying other methods to the images shown in Fig. 8. a and Fig. 10. a. Fig. 9. a shows the results of a closed-form matting method [8]. Fig. 9. b shows the results of an object segmentation method [10], and Fig. 9. c shows the results of a k-means method. Compared with our methods, these results are considerably less accurate and less robust. For these experiments, we used the Interactive Segmentation Tool-Box software (<http://www.cs.cmu.edu/mohit/segmentation.htm>) and matting software [8].

Finally, we conducted experiments simulating color change depending on various thicknesses of the top layer. Fig. 10 shows the simulation results for a number of real objects using our method. In each image, (a) is the input image, and (b) is the estimated opacity image.

Fig. 10. 1 shows the results of Fig. 8. In these results, we can simulate color change by various thicknesses of pigments. Fig. 10. 2 shows the results of a rock painting using powdered mineral pigments. We tried to recover some of the degraded parts of the wall painting. From the results, we could simulate color changes based on the various degrees of degradation. Fig. 10. 3 shows a relief of an ancient

temple that was degraded by microorganisms. Using these simulation results, it is possible to show the degree of microbial growth.

7. Discussions

In this discussion, we intend to explain the reasons we use the LB-based model instead of using the KM model. The latter model is expressed as:

$$I_c = \frac{\frac{1}{F_c}(B_c - F_c) - F_c(B_c - \frac{1}{F_c})e^{SX(\frac{1}{F_c}) - F_c}}{(B_c - F_c) - (B_c - \frac{1}{F_c})e^{SX(\frac{1}{F_c} - F_c)}} \quad (19)$$

where X is the thickness, S is the scattering coefficient. As one can observe, the equation is considerably more complex compared to that of the LB-based model.

Aside from the complexity of the model, we have intensive empirical comparisons between the two models. For this, we hold the following expectation: For a given top layer with a certain opacity on top of several different bottom layers, the estimated F_c must be consistent. With this expectation, we compared the accuracy and robustness of the KM and the LB-based model.

We experimented with various transparent objects as the top layers and various opaque objects as the bottom layer. We calculated RMSE (Root mean square error) and STD (standard deviation) w.r.t the ground truth. For the KM model, the RMSE was 0.2993, and the STD was 0.0247. For the LB-based model, the RMSE was 0.2964, and the STD was 0.0273. These results show that the accuracy difference of the KM and LB-based models was insignificant. Therefore, it is reasonable to choose the LB-based model over the KM model due to the simplicity of the former model. Note that, like the KM model, the LB-based model assumes that the scattering coefficients are considerably small and negligible.

Our framework is capable of both decomposing layered surfaces and simulating the image of layered surfaces efficiently. We consider that the framework can be useful for many applications. First, we mentioned opacity simulations, which can be useful for computer graphics. Second, in water color paintings, we can apply our framework for color editing. Finally, in wall paintings, we can recover original regions of the degraded wall painting, and also analyze the process of degradation.

8. Conclusions

We have demonstrated a decomposition method for layered surfaces by using the spider model, a novel model to analyze the distribution of layered surface in the RGB space. The decomposition is equivalent to extracting the optical properties of the surfaces. We consider the process of decomposing layered surfaces could benefit many applications in computer vision and graphics, since many objects in

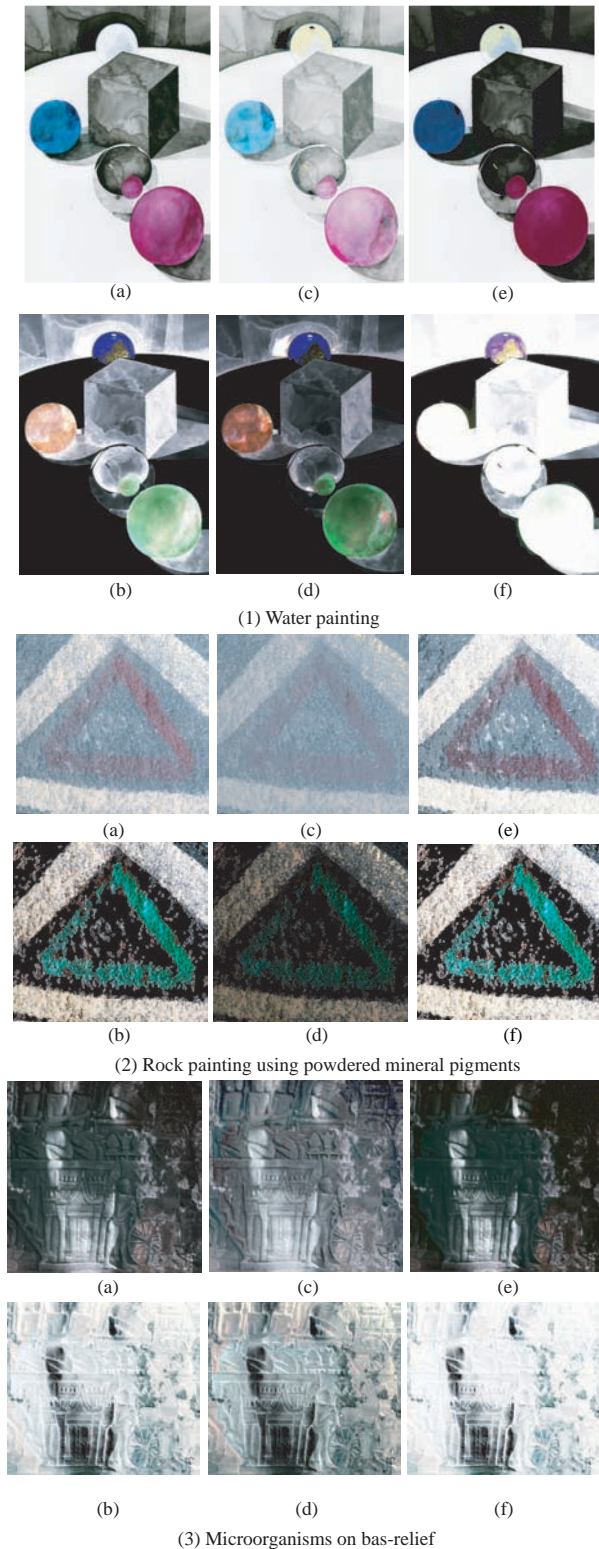


Figure 10. Simulating color change of layered surfaces depending on various thicknesses of top Layers. (a) Input image. (b) Estimated opacity $1 - e^{-\mu d}$ image. (c) Simulated image by reducing the opacity 10%. (d) Opacity image reduced 10%. (e) Simulated image increasing opacity 3 times. (f) Opacity image increased 3 times.

nature have layered surfaces. In addition, experiments with real images showed the effectiveness and the robustness of our proposed method.

References

- [1] A. Beer. Bestimmung der absorption des rothen lichts in farbigen flussigkeiten. *Ann. Phys. Chem.*, 86(2):78–90, 1852. [2](#)
- [2] M. Born and E. Wolf. *Principles of Optics*. Cambridge, seventh edition, 1999. [2](#)
- [3] S. Chandrasekhar. *Radiative Transfer*. Dover, New York, 1960. [2](#)
- [4] Y. Chuang, B. Curless, D. Salesin, and R. Szeliski. A bayesian approach to digital matting. *CVPR*, 2001. [2](#)
- [5] R. Fattal. Single image dehazing. *SIGGRAPH*, 2008. [2](#)
- [6] A. Ishimaru. *Wave propagation and scattering in random media*. IEEE Press and Oxford University Press, New York, 1999. [2](#)
- [7] P. Kubelka and F. Munk. Ein beitrage zur optik der farbanstriche. *Z. Tech. Phys.*, 12:593–601, 1931. [2](#)
- [8] A. Levin, D. Lischinski, and Y. Weiss. A closed form solution to natural image matting. *CVPR*, 2006. [2, 7](#)
- [9] A. Levin, A. Rav-Acha, and D. Lischinski. Spectral matting. *CVPR*, 2007. [2](#)
- [10] Y. Li, J. Sun, C. Tang, and H. Shum. Lazy snapping. *ACM Trans. on Graphics*, 23:303–308, 2004. [7](#)
- [11] P. Mudgett and L. Richard. Multiple scattering calculations for technology. *Applied Optics*, 10(7):1485–1502, 1971. [2](#)
- [12] S. Narasimhan and S. Nayar. Interactive deweathering of an image using physical models. *IEEE Workshop on Color and Photometric Method in Computer Vision*, 2003. [2](#)
- [13] S. K. Nayar and S. G. Narasimhan. Vision in bad weather. In *ICCV (2)*, pages 820–827, 1999. [2, 3](#)
- [14] I. Omer and M. Werman. Color lines: Image specific color representation. *CVPR*, 2004. [4](#)
- [15] R.T.Tan. Visibility in bad weather from a single image. *CVPR*, 2008. [2](#)
- [16] M. Ruzon and C. Tomashi. Alpha estimation in natural images. *CVPR*, pages 18–25, 2000. [2](#)
- [17] Y. Schechner and N. Karpel. Clear underwater vision. *CVPR*, 2004. [2](#)
- [18] J. Sun, J. Jia, C. Tang, and H. Shum. Poisson matting. in *proceedings of SIGGRAPH*, 2004. [2](#)
- [19] R. Szeliski, R. Zabih, D. Scharstein, O. Veksler, V. Kolmogorov, A. Agarwala, M. Tappen, , and C. Rother. A comparative study of energy minimization methods for markov random fields. *ECCV*, 2006. [6](#)
- [20] J. Wang and M. Cohen. An iterative optimization approach for unified image segmentation and matting. *ICCV*, 2005. [2](#)
- [21] G. Wyszecki and W. Stiles. *Color Science: Concept and Methods, Quantitative Data and Formulae*. Wiley Inter-Science, second edition, 1982. [2](#)